# Observation of Griffiths Phase in Polycrystalline $La_{1-x}Ca_xMnO_3$ for $x \sim 0.20$

Hongguang Zhang, Qi Li, Hao Liu, Lingshan Chen, Yuanyuan Chen, and Yongtao Li

Department of Physics, Southeast University, Nanjing, 211189, P. R. China

**Polycrystalline samples $La_{1-x}Ca_xMnO_3$ have been prepared by sol-gel method. X-ray diffraction patterns show that all the samples are mostly in single phase. Magnetic properties have been measured by Quantum Designed Physical Properties Measurement System. From the measured $M - T$ curves, the samples show a traditional paramagnetic-to-ferromagnetic phase transition near Curie temperature. The Griffiths phase is found in all the samples from the temperature dependence curves of inverse susceptibility even for the samples with doping concentrations lower than 0.20 (the terminated doping concentration of Griffiths phase in single crystal $La_{1-x}Ca_xMnO_3$). A conclusion is summarized that the existence of Griffiths phase depends on whether the sample is single crystal or polycrystalline one.**

*Index Terms*—**Magnetic susceptibility, magnetoresistance, manganese compounds, polycystalline.**

## I. INTRODUCTION

COLOSSAL MAGNETO-RESISTANCE (CMR) materials have been focused for a long time since their latent applications in terms of magnetic storage and magnetic tip [1]. As we all know, doped manganites with the general formula $RE_{1-x}AE_xMnO_3$ (where RE is rare earth and AE is alkaline earth) are the typical and basic materials with the CMR effect, especially for $La_{1-x}Ca_xMnO_3$. Many models have been proposed to explain these physical phenomena, such as Double exchange (DE) interaction [2], electron-phonon interaction intrigued by Jahn-Teller distortion [3], polaron model [4], phase separation [5], and percolative phase transition [6], [7]. However, there is no unique model to understand manganites, which means a further investigation is still needed.

Recently, Griffiths phase has been proposed to explain the CMR effect. In 2002, Salamon *et al.* thought Griffiths phase is the prerequisite of CMR [8] and they also proved that the CMR effect is a Griffiths singularity [9]. However, Jiang *et al.* [10] had found that there is no Griffiths phase in single crystal $La_{0.80}Ca_{0.20}MnO_3$, although the CMR effect exists in this sample. More work [10]–[12] found that non-Griffiths-like phase is present in different samples with CMR effect, even though the same parent with distinct doping ions. Therefore, the relationship between CMR and Griffiths phase has been suspected.

As to the disparate doping concentration of non-Griffiths-like phase in doped manganites, polycrystalline $La_{1-x}Ca_xMnO_3$ ($x = 0.19, 0.20, 0.21$) have been studied to investigate whether there is Griffiths phase in polycrystalline even for the concentration $x$ lower than the terminated doping concentration of Griffiths phase in single crystal sample $La_{1-x}Ca_xMnO_3$ ($x = 0.20$).

## II. EXPERIMENTAL DETAILS

The polycrystalline samples used in the present study, with a nominal composition $La_{1-x}Ca_xMnO_3$ ($x = 0.21, 0.20, 019$), were prepared by sol-gel method with the high pure $La_2O_3$, $Ca(NO_3)_2$, $Mn(NO_3)_2$. The mixture was heated in air at 1000 °C for 30 hours, then cooled down to room temperature in the furnace. The phase purity of our samples was checked by powder X-ray diffraction (XRD) using $Cu\ K\alpha$ radiation at room temperature. In Fig. 1, the bottom curve is the standard XRD pattern of $La_{0.8}Ca_{0.2}MnO_3$, which comes from an inorganic crystal structure database-NIST/FIZ. Compared with it, the XRD patterns of our samples show that they are mostly in single phase although a few tiny peaks of additional phases are found. According to Scherrer function ($D = 0.89\lambda/d\cos\theta$), grain size were given 84.0 nm, 70.9 nm, 63.4 nm, for $x = 0.19$, 0.20, 0.21, respectively. The other corresponding lattice parameters were given in Table I using least square method and Bragg formula. The magnetization was measured by Quantum Design Physical Properties Measurement System (PPMS) with 100 Oe magnetic fields in the temperature range of 77–300 K. X-ray absorption fine structure (XAFS) at the Mn $K$ edge of three of our samples were performed at room temperature at the National Synchrotron Radiation Laboratory (NSRL), University of Science and Technology of China (USTC). The XAFS signals of $LaMnO_3$ and $CaMnO_3$ samples were also recorded for comparison. The energy range of the monochromatized X-rays was 4–13.5 KeV provided by a double crystal monochromator using Si(111). The normalized X-ray absorption near edge structure (XANES) spectra was obtained after background subtraction.

## III. RESULTS AND DISCUSSION

Temperature dependence of magnetization is shown in Fig. 2. The samples given show a traditional transition from Paramagnetic phase (PM) to Ferromagnetic phase (FM). Because of the coupling of the oxygen 2p holes with the $3d^4$ local moments on $Mn^{3+}$ ions, the moments align ferromagnetically. In the low-temperature range, the samples show ferromagnetism and

TABLE I
ALL THE PARAMETERS GIVEN BY FITTING EXPERIMENTAL DATA. ($T_C$ IS THE CURIE TEMPERATURE; $T_G$ IS A CHARACTERISTIC TEMPERATURE OF GRIFFITHS PHASE; $T_C^*$ AND $\lambda$ ARE THE FITTED PHYSICAL QUANTITY BASED ON THE RELATIONSHIP (2) (SEE CONTEXT); $S_{\text{eff}}$ IS THE FITTED VALUE OF EFFECTIVE SPIN FROM THE EXPERIMENTS AND $S_{\text{eff}}^*$ IS THE THEORY CALCULATED VALUE; THE LATTICE PARAMETERS $a, b, c$ ARE SHOWN IN THE LAST THREE PANE IN THE TABLE)

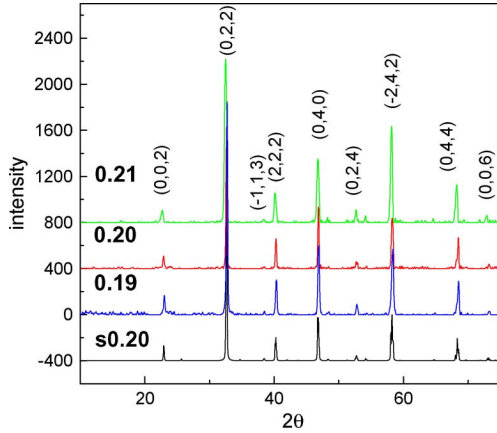| Sample ($x$) | $T_C$ (K) | $T_G$ (K) | $T_C^*$ (K) | $S_{eff}$ | $S^*_{eff}$ | $\lambda$ | Grain Volume (nm) | $a$ (nm) | $b$ (nm) | $c$ (nm) |
|---|---|---|---|---|---|---|---|---|---|---|
| 0.19 | 231.3 | 271.0 | 257.25 | 4.33 | 1.905 | 0.487 | 0.46322 | 0.7737 | 0.7735 | 0.7740 |
| 0.20 | 224.1 | 243.8 | 233.81 | 5.30 | 1.900 | 0.271 | 0.46373 | 0.7736 | 0.7739 | 0.7746 |
| 0.21 | 213.6 | 261.5 | 248.03 | 4.59 | 1.895 | 0.564 | 0.46701 | 0.7753 | 0.7760 | 0.7763 |



Fig. 1. X-ray diffraction patterns of $La_{1-x}Ca_xMnO_3$ samples. The bottom line (s0.20) represents the standard XRD pattern of $La_{0.8}Ca_{0.2}MnO_3$. The measuring range ($2\theta$) of all the patterns is from $10°$ to $75°$.
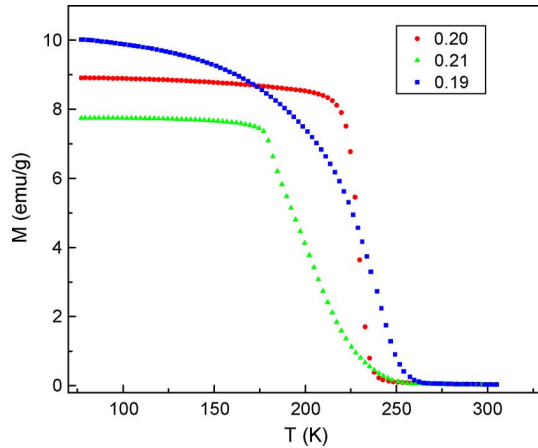


Fig. 2. Temperature dependence of magnetization of $La_{1-x}Ca_xMnO_3$ samples. Magnetization measurement was performed for the samples on heating in a low field of 100 Oe after cooling in the field (FC). The square, solid circle and triangle represent the magnetization curve of 0.19, 0.20, 0.21, respectively.

their saturated magnetization decreases with the doping concentration increasing. This can be explained from the relationship between structure and magnetism. As is known, the structure of manganites is governed by tolerance factor $t = (r_A + r_O)/\sqrt{2}(r_B + r_O)$. The perovskite structure is stable for $0.89 < t < 1.02$. For hole-doped manganites system [13], a decrease of $t$ bends the Mn-O-Mn band angle from $180°$ and enhances the buckling effect, which decreases the effective $e_g$ electron hopping kinetic energy $E_{\text{eff}}$. A sufficiently small value of $E_{\text{eff}}$ leads to the strong localization of electrons by the competing

electron-phonon interaction. Based on the DE mechanism, the localization of the electrons is adverse to the FM interaction and the ferromagnetism is enhanced along with tolerance factor $t$ increasing. For our samples, the increasing of concentration $x$ signifies the decreasing of tolerance factor $t$. Thus, the decreasing of their saturated magnetization with $x$ increasing is reasonable.

The high-temperature part of magnetization curves follows Curie–Weiss law, indicating paramagnetic phase at this temperature range. For this part, we use Curie–Weiss law to fit the experimental data according to the inverse-susceptibility versus temperature in Fig. 3

$$\chi^{-1} = \frac{3k_B T_C}{Ng^2\mu_B^2 S_{\text{eff}}(S_{eff}+1)}\left(\frac{T}{T_C} - 1\right) \qquad (1)$$

where $S_{\text{eff}}$ is the effective spin, $g$ is the Lande factor, $\mu_B$ is the Bohr magneton, $T_C$ is the Curie Temperature. Curie temperature has been determined by extrapolating the paramagnetic part of the inverse susceptibility. Curie temperature and Griffiths temperature are shown in Table I. All Curie temperatures are higher than that of single crystal [14] and consistent with the values in literature [15]. Moreover, the estimated values of $S_{\text{eff}}$ in all samples are larger than that of theoretical $S_{\text{eff}}^*$, for an effective Mn ion (the weighted average of $S_{\text{Mn}^{3+}} = 2$ and $S_{\text{Mn}^{4+}} = 3/2$). This indicates that the magnetism of the PM state of the samples includes the contributions of short range clusters which are supplied by not only the Mn ion but also other kinds of interplay interaction [16]. This interplay interaction refers to the formation of $\text{Mn}$ dimmers [17] with the changes of local structure. Thus, this larger effective spin can be explained by the accumulation of such local dimerons which is constrained by the quenched disorder of the $\text{Ca}^{2+}$ doping. As is known, J. Burgy, et al. [18] proposed that a competition between two ordered states in the presence of quenched disorder is in favor of the formation of Griffiths phase. The existence of short range clusters in our samples means the magnetic inhomogeneities in PM state, thus it can be concluded that Griffiths phase may exist in all our samples. Temperature dependence of inverse-susceptibility is the key tool to demonstrate it. From the fitting curve in the paramagnetic region, we can observe that the $H/M$ deviates from the Curie–Weiss law below a corresponding temperature. This is regarded as a new phase caused by quenched disorder—Griffiths phase.

Based on Griffiths' theory, Griffiths phase in the pioneering work is pointed out on a random Ising ferromagnet, which is definitely demonstrated by Bray [19]–[21]. One of the characteristics of Griffiths phase is a sharp downturn in the inverse
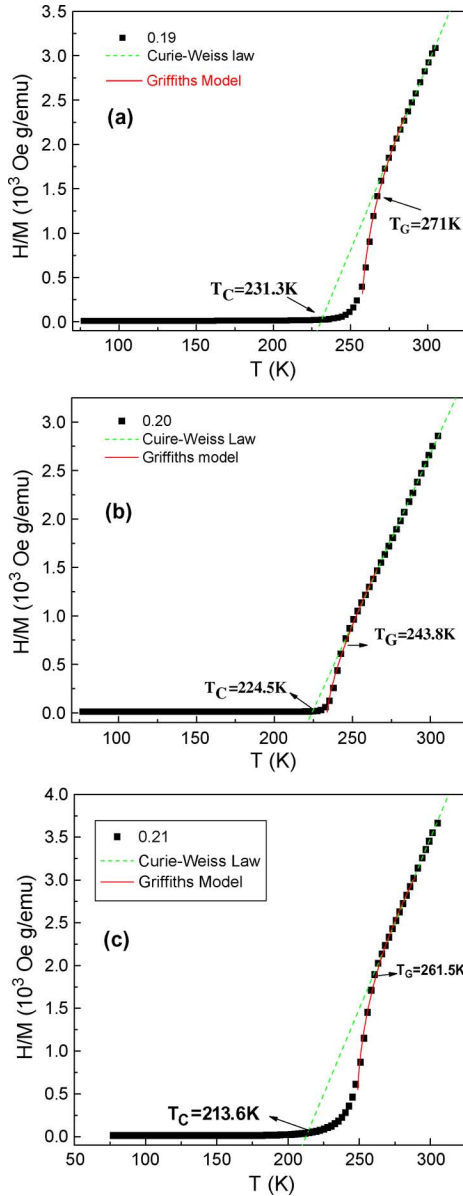
Fig. 3. Temperature dependence of the inverse susceptibility for all $La_{1-x}Ca_xMnO_3$ samples (the signals ╱ and the dash lines denote the Curie temperature, Griffiths temperature and the fitting curve with the Curie–Weiss law, respectively. The solid curve denotes the fitting curve with Griffiths model).



Fig. 4. The normalized Mn $K$-edge XANES spectra at room temperature for $LaMnO_3$, $La_{0.81}Ca_{0.19}MnO_3$, $La_{0.80}Ca_{0.20}MnO_3$, $La_{0.79}Ca_{0.21}MnO_3$, $CaMnO_3$ samples. The inset shows the enlarged image of the spectra of our three samples.

of high-temperature susceptibility above $T_C$ [10]. As is shown in Fig. 3, a sharp downturn appearing in all samples means the existence of Griffiths phase. According to [10], [11], there is no Griffiths phase found in single crystal $La_{0.80}Ca_{0.20}MnO_3$ and this doping concentration is the terminated doing concentration of Griffiths phase. Therefore, the results above prove that Griffiths phase occurs even for the polycrystalline samples with doping concentrations lower than 0.20. From the observation of Griffiths phase in our sample $x = 0.20$, it demonstrates that the existence of Griffiths phase has a great dependence on whether samples are single crystal or polycrystalline one. Importantly, the Griffiths phase even exists in the sample $x = 0.19$, whether it exists in single crystal samples has not been reported yet. As reported, doping concentration 0.20 is the terminated concentration of Griffiths phase in single crystal $La_{1-x}Ca_xMnO_3$ [11],
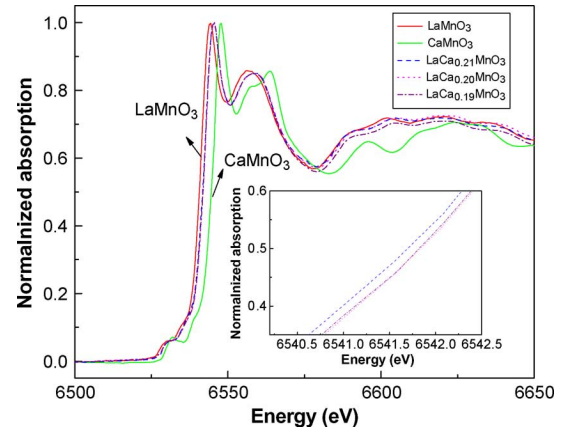
that is, non-Griffiths-like phase exists in the single crystal with doping concentration lower than 0.20. And it has been reported recently that the polycrystalline sample $La_{0.875}Ca_{0.125}MnO_3$ has no Griffiths phase above its Curie temperature [22]. Thus, the nature of the occurrence of Griffiths phase both in single crystal and in polycrystalline samples is totally different in this system.

Based on the Griffiths' theory and Bray's perspective [19]–[21], the Griffiths regime shows neither the traditional paramagnetism nor an infinite percolating chain. It is established by largest cluster and correlated volume. The following relationship is an appropriate prediction to the Griffiths phase:

$$\chi^{-1}(T) \propto (T - T_C^*)^{1-\lambda} \qquad (0 < \lambda < 1) \qquad (2)$$

In order to further investigate the Griffiths phase in our samples, the experimental data were fitted according to the relation above. The solid line in Fig. 3 is the fitting curves, which is the so-called Griffiths model. The exponent $\lambda$ is a parameter which relates strongly with Griffiths phase. The fitting parameters $\lambda$ and $T_C^*$ are listed in Table I. $\lambda$ in the sample $x = 0.21$ is 0.564 (viz. $\lambda_p = 0.564$) which is a little larger than that in single crystal ($\lambda_s = 0.31$) [10]. The difference of the two values ($\Delta\lambda(p - s) = \lambda_p - \lambda_s = 0.254$) indicates the enhancement of a Griffiths phase. Interestingly, this difference is consistent with the $\lambda$ value (0.271) in the sample $x = 0.20$. This is a possible reason of the appearance of Griffiths phase in polycrystalline but not in single crystal $x = 0.20$. A conclusion can be summarized that the larger lattice disorder in polycrystalline can enhance the Griffiths phase compared with single crystals. As to $x = 0.19$, the small value of $\lambda$ (0.487) relative to $x = 0.21$ is inclined to the diminution of a Griffiths phase.

For the purpose to investigate the essential difference of Griffiths phase in all the samples, XAFS spectra have been measured at the NSRL, USTC. Normalized XANES spectra at the Mn $K$ edge of the $La_{1-x}Ca_xMnO_3$ ($x = 0.19, 0.20, 0.21$) series at room temperature are shown in Fig. 4. The threshold energies ($E_0$) obtained from the inflection point of the edge are listed in Table II. From the Fig. 4, it can be seen that the three

| Compound | $E_0$ (eV) |
|---|---|
| $LaMnO_3$ | 6540.82 |
| $La_{0.81}Ca_{0.19}MnO_3$ | 6541.58 |
| $La_{0.80}Ca_{0.20}MnO_3$ | 6542.05 |
| $La_{0.79}Ca_{0.21}MnO_3$ | 6541.55 |
| **$CaMnO_3$** | 6544.39 |

curves are mostly the same as each other and no obvious distinction is found. As is known, the pre-edge region is related with transition to empty Mn d-states due to the hybridization with the adjacent oxygen p-states, and the main-edge region is corresponding to dipolar transitions to the empty Mn p-band. Therefore, the local electronic structure has no large difference at room temperature in all our samples. The absorption spectra of our samples are shown between $LaMnO_3$ and $CaMnO_3$, which indicates a mixed valance state for manganese. This result is consistent with the report in [23], [26]. However, only this chemical shift cannot differentiate the two kinds of manganese atoms ($Mn^{3+}$ and $Mn^{4+}$). Obviously, this mixed valence state is definitely caused by the dopant ion $Ca^{2+}$. From the large effective spin in this paper, we propose that there is an intrinsic inhomogeneous distribution of the mixed valance state for manganese. Based on the relation between quenched disorder caused by A-site cation doping and the formation of a Griffiths phase, the inhomogeneous distribution of mixed valence Mn ions probably is the main factor of the occurrence of Griffiths phase. From the above mentioned, the crystal form of samples (single crystal or polycrystalline sample) has a crucial effect on the occurrence of Griffiths phase.

## IV. CONCLUSION

In summary, we have prepared polycrystalline samples $La_{1-x}Ca_xMnO_3$ by sol-gel method. All the samples are in single phase, as is shown by XRD patterns. From the measured $M - T$ curve, the samples show a traditional paramagnetic-to-ferromagnetic phase transition near Curie temperature. Griffiths phase is found in all the samples from inverse susceptibility-temperature curve even for the samples with doping concentrations lower than the Griffiths phase terminated doping concentration 0.20. A conclusion is deduced that the existence

of Griffiths phase is related to whether the sample is single crystal or polycrystalline one. XANES spectra at room temperature indicate that no large difference of local electronic structure occur in our samples.

## REFERENCES

[1] H. B. Lu, S. Y. Dai, and Z. H. Chen *et al., Appl. Phys. Lett.*, vol. 86, p. 032502, 2005.
[2] C. Zener, *Phys. Rev.*, vol. 82, p. 403, 1995.
[3] D. Feinberg *et al., Phys. Rev. B*, vol. 57, p. R5583, 1998.
[4] A. Lanzara, N. L. Saini, M. Brunelli, and F. Natali *et al., Phys. Rev. Lett.*, vol. 81, p. 878, 1998.
[5] M. Uehara, S. Mori, C. H. Chen, and S.-W. Cheong, *Nature*, vol. 399, p. 560, 1999.
[6] A. Moreo, S. Yunoki, and E. Dagotto, *Science*, vol. 283, p. 2034, 1999.
[7] E. Dagotto, T. Hotta, and A. Moreo, *Phys. Rep.*, vol. 344, p. 1, 2001.
[8] M. B. Salamon and P. Lin, *Phys. Rev. Lett.*, vol. 88, p. 197203, 2002.
[9] M. B. Salamon, *Phys. Rev. B*, vol. 68, p. 014411, 2003.
[10] W. J. Jiang, X. Z. Zhou, and G. Williams *et al., Phys. Rev. Lett.*, vol. 99, p. 177203, 2007.
[11] W. J. Jiang, X. Z. Zhou, and G. Williams, *Phys. Rev. B*, vol. 77, p. 064424, 2008.
[12] C. He, M. A. Torija, and C. Leighton *et al., Phys. Rev. B*, vol. 76, p. 014401, 2007.
[13] H. Y. Hwang, S.-W. Cheong, P. G. Radaelli, M. Marezio, and B. Batlogg, *Phys. Rev. Lett.*, vol. 75, p. 914, 1995.
[14] R. I. Zainullina, N. G. Bebenin, and V. V. Ustinov *et al., Phys. Rev. B*, vol. 76, p. 014408, 2007.
[15] C. H. Booth, F. Bridges, G. H. Kwei, J. M. Lawrence, A. L. Cornelius, and J. J. Neumeier, *Phys. Rev. Lett.*, vol. 80, p. 853, 1998.
[16] C. L. Lu, K. F. Wang, S. Dong, J. G. Wan, and J. M. Liu, *J. Appl. Phys.*, vol. 103, p. 07F714, 2008.
[17] L. Downward, F. Bridges, S. Bushart, J. J. Neumeier, N. Dilley, and L. Zhou, *Phys. Rev. Lett.*, vol. 95, p. 106401, 2005.
[18] J. Burgy, M. Mayr, V. Martin-Mayor, A. Moreo, and E. Dagotto, *Phys. Rev. Lett.*, vol. 87, p. 2772021, 2001.
[19] R. B. Griffiths, *Phys. Rev. Lett.*, vol. 23, p. 17, 1969.
[20] A. J. Bray and M. A. Moore, *J. Phys. C*, vol. 15, p. L765, 1982.
[21] A. J. Bray, *Phys. Rev. Lett.*, vol. 59, p. 586, 1987.
[22] E. Bose, S. Karmakar, B. K. Chaudhuri, S. Pal, C. Martin, S. Hébert, and A. Maignan, *J. Phys. D: Appl. Phys.*, vol. 40, p. 3728, 2007.
[23] G. Subías, J. García, M. G. Proietti, and J. Blasco., *Phys. Rev. B*, vol. 56, p. 8183, 1997.
[24] K. H. Kim, J. Y. Gu, H. S. Choi, G. W. Park, and T. W. Noh, *Phys. Rev. Lett.*, vol. 77, p. 1877, 1996.
[25] J. M. De Teresa *et al., Nature*, vol. 386, p. 256, 1997.
[26] M. Croft, D. Sills, M. Greenblatt, C. Lee, S.-W. Cheong, K. V. Ramanujachary, and D. Tran, *Phys. Rev. B*, vol. 55, p. 8726, 1997.